

# Orbital Magnetism and Current Distribution of Two-Dimensional Electrons under Confining Potential

Yasushi ISHIKAWA\* and Hidetoshi FUKUYAMA

*Department of Physics, University of Tokyo, Tokyo 113-0033*

(Received October 17, 2018)

The spatial distribution of electric current under magnetic field and the resultant orbital magnetism have been studied for two-dimensional electrons under a harmonic confining potential  $V(\mathbf{r}) = m\omega_0^2 r^2/2$  in various regimes of temperature and magnetic field, and the microscopic conditions for the validity of Landau diamagnetism are clarified. Under a weak magnetic field ( $\omega_c \lesssim \omega_0$ ,  $\omega_c$  being a cyclotron frequency) and at low temperature ( $T \lesssim \hbar\omega_0$ ), where the orbital magnetic moment fluctuates as a function of the field, the currents are irregularly distributed paramagnetically or diamagnetically inside the bulk region. As the temperature is raised under such a weak field, however, the currents in the bulk region are immediately reduced and finally there only remains the diamagnetic current flowing along the edge. At the same time, the usual Landau diamagnetism results for the total magnetic moment. The origin of this dramatic temperature dependence is seen to be in the multiple reflection of electron waves by the boundary confining potential, which becomes important once the coherence length of electrons gets longer than the system length. Under a stronger field ( $\omega_c \gtrsim \omega_0$ ), on the other hand, the currents in the bulk region cause de Haas-van Alphen effect at low temperature as  $T \lesssim \hbar\omega_c$ . As the temperature gets higher ( $T \gtrsim \hbar\omega_c$ ) under such a strong field, the bulk currents are reduced and the Landau diamagnetism by the edge current is recovered.

KEYWORDS: orbital magnetism, confining potential, Landau diamagnetism, edge current, multiple reflection, mesoscopic system

## §1. Introduction

Bohr-van Leeuwen's theorem tells us that the orbital magnetism does not appear in classical theory.<sup>1,2)</sup> The physical argument for this fact is that the diamagnetic current due to cyclotron orbits of electrons in the bulk region is perfectly cancelled by the paramagnetic current due to skipping orbits near the boundary. The orbital magnetism, which is then possible only in quantum mechanics, was originally derived based on the Landau levels.<sup>3)</sup> In the actual derivation, effects of the boundary have not been taken into account explicitly. These effects of boundary on the

---

\* E-mail: ishikawa@watson.phys.s.u-tokyo.ac.jp

orbital magnetism have been later investigated by many authors<sup>.4,5,6,7,8,9,10,11,12,13,14,15)</sup> Above all, Kubo<sup>4)</sup> has applied the Wigner representation to an electron system under a magnetic field and shown that, if a confining potential is slowly varying in space compared to the electron wave length, the Landau diamagnetism results. However, this treatment is not valid at low temperature as stressed by Kubo and clear from the expansion parameters. The magnetic moment at  $T = 0$ , on the other hand, has been shown by Denton<sup>7)</sup> and Nemeth<sup>11)</sup> to be different from the Landau diamagnetism in a system under a harmonic confining potential. Yoshioka and Fukuyama<sup>14)</sup> has actually indicated that under a weak field and at low temperature ( $k_B T \lesssim$  energy spacing by a confinement), the magnetic moment of the whole system shows a large fluctuation, and as the temperature is raised under such a weak field, fluctuations disappear and Landau diamagnetism is recovered. Hajdu and Shapiro<sup>15)</sup> pointed out by studying the case of a groove with a width  $L$  that the temperature below which such fluctuations appear is such that  $k_B T \sim \hbar/\tau_{tr}$  where  $\tau_{tr} = L/v_F$ , the time of flight for electrons at the Fermi energy across the system. Stimulated by these indications, we will study in this paper the spatial distribution of current in a confined system in order to understand more details of such a variety of orbital magnetism. From the investigations so far, the shape of confining potential, whether it is harmonic or hard wall, is expected not to affect qualitative aspects of the characteristic features of the orbital magnetism. Therefore we assume a harmonic potential which makes the analytical studies possible, and then clarify the relationship between the orbital magnetism and the spatial distribution of current in various regimes of temperature and magnetic field.

The organization of this paper is as follows. In §2, we introduce the model and summarize the general feature of the orbital magnetic moment. In §3, the spatial distribution of current will be studied in various regions of temperature and magnetic field, and the microscopic conditions for the validity of Landau diamagnetism are clarified. Summary is given in §4.

We take units  $k_B = 1$  in the following.

## §2. Magnetic Moment of Two-Dimensional Confined System

In this section, we introduce our model and explain the general properties of the magnetic moment of the system. We consider two-dimensional electrons confined by an isotropic harmonic potential and the magnetic field is applied perpendicular to the system. For simplicity, we consider spinless electrons with the total number  $N_0$  and neglect Coulomb interactions between them. We assume  $N_0$  is large enough that the difference between a grand canonical ensemble and a canonical one is of no importance and rely on a grand canonical one to derive a magnetic moment. The word “magnetic moment” in this paper implies a magnetic moment of the whole system.

The Hamiltonian is written as

$$\mathcal{H} = \frac{1}{2m} \left( \mathbf{p} + \frac{e}{c} \mathbf{A} \right)^2 + \frac{1}{2} m \omega_0^2 \mathbf{r}^2, \quad (2.1)$$

where  $\mathbf{p}$  and  $\mathbf{r}$  are two-dimensional vector,  $m$  is the electron mass and  $(-e)$  is the electron charge. The radius of the system,  $R$ , is classically defined as

$$\frac{1}{2}m\omega_0^2 R^2 = \mu, \quad (2.2)$$

where  $\mu$  is the chemical potential.

By taking a symmetric gauge  $\mathbf{A} = \frac{1}{2}\mathbf{H} \times \mathbf{r}$ , we can obtain an eigenfunction diagonal with respect to the angular momentum  $\alpha$  as

$$\begin{aligned} \psi_{n\alpha}(\mathbf{r}) &= \frac{e^{i\alpha\theta}}{\sqrt{2\pi}} R_{n\alpha}(r) \\ R_{n\alpha}(r) &= \frac{1}{l} \sqrt{\frac{n!}{(n+|\alpha|)!}} \exp\left[-\frac{r^2}{4l^2}\right] \left(\frac{r}{\sqrt{2}l}\right)^{|\alpha|} L_n^{(|\alpha|)}\left[\frac{r^2}{2l^2}\right] \end{aligned} \quad (2.3)$$

where polar coordinates  $(r, \theta)$  are used, and  $n = 0, 1, 2, \dots$ ,  $\alpha = 0, \pm 1, \pm 2, \dots$  and  $l = \sqrt{\hbar/m\omega}$ ,  $\omega = \sqrt{\omega_c^2 + (2\omega_0)^2}$ ,  $\omega_c = eH/mc$  being the cyclotron frequency and  $L_n^{(\alpha)}$  is the Laguerre polynomial. The eigenenergy of this state,  $E_{n\alpha}$ , is given by

$$E_{n\alpha} = \hbar\omega_c \frac{\alpha}{2} + \hbar\omega \left(n + \frac{|\alpha| + 1}{2}\right). \quad (2.4)$$

Especially under a extremely strong field ( $\omega_c \gg \omega_0$ ), this eigenenergy  $E_{n\alpha}$  becomes  $\hbar\omega_c(n + 1/2)$  for negative  $\alpha$ . So, the quantum number  $n$  corresponds to the Landau level index.

By use of eq. (2.4), the thermodynamic potential  $\Omega$  is written as

$$\Omega = -\frac{1}{\beta} \sum_{n=0}^{\infty} \sum_{\alpha=-\infty}^{\infty} \log \left[ 1 + e^{-\beta(E_{n\alpha} - \mu)} \right], \quad (2.5)$$

where  $\beta = 1/T$  and  $\mu$  is the chemical potential adjusted to fix the average electron number to  $N_0$  at each values of  $H$  and  $T$ .

From the thermodynamic potential, the magnetic moment  $M$  is given as

$$\begin{aligned} M &= -\left(\frac{\partial\Omega}{\partial H}\right)_{\mu} \\ &= \sum_{n\alpha} \left(-\frac{\partial E_{n\alpha}}{\partial H}\right) f(E_{n\alpha}) \end{aligned} \quad (2.6)$$

where  $f(E)$  is the Fermi distribution function.

Applying the Poisson summation formula<sup>21)</sup> to the sum over  $n$  and  $\alpha$  in eq. (2.5) (for details, see Appendix A), one obtains

$$\Omega = \Omega_0 + \Omega_L + \Omega_{osc}, \quad (2.7)$$

where

$$\Omega_0 = -\frac{1}{\beta(\hbar\omega_0)^2} \int_0^{\infty} d\varepsilon \int_0^{\infty} d\eta \log \left[ 1 + e^{-\beta(\varepsilon + \eta - \mu)} \right] + \frac{1}{12} \mu, \quad (2.8)$$

$$\Omega_L = \frac{1}{24} \left( \frac{\omega_c}{\omega_0} \right)^2 \mu, \quad (2.9)$$

$$\begin{aligned} \Omega_{osc} \simeq & \frac{1}{2\pi\beta} \sum_{k=1}^{\infty} (-1)^k \left[ \left( \frac{\omega}{\omega_0} \right)^2 \frac{1}{k^2} - \frac{\pi^2}{3} \right] \frac{\sin(2\pi k\mu/\hbar\omega)}{\sinh(2\pi^2 k/\beta\hbar\omega)} \\ & + \frac{1}{2\pi\beta} \sum_{\sigma=\pm} \sum_{l=1}^{\infty} \left( \frac{\omega_{\sigma}}{\omega} \right) \frac{1}{l^2} \frac{\sin(2\pi l\mu/\hbar\omega_{\sigma})}{\sinh(2\pi^2 l/\beta\hbar\omega_{\sigma})} \\ & + \frac{1}{\pi\beta} \sum_{\sigma=\pm} \sum_{k=1}^{\infty} \sum_{l=1}^{\infty} \frac{(-1)^k}{l} \left[ \frac{\sin\left[\frac{\pi\mu}{\hbar\omega} \left(k - \frac{\omega}{\omega_{\sigma}} l\right)\right] \cos\left[\frac{\pi\mu}{\hbar\omega} \left(k + \frac{\omega}{\omega_{\sigma}} l\right)\right]}{\left(k - \frac{\omega}{\omega_{\sigma}} l\right) \sinh(2\pi^2 l/\beta\hbar\omega_{\sigma})} \right. \\ & \left. + \frac{\sin\left[\frac{\pi\mu}{\hbar\omega} \left(k + \frac{\omega}{\omega_{\sigma}} l\right)\right] \cos\left[\frac{\pi\mu}{\hbar\omega} \left(k - \frac{\omega}{\omega_{\sigma}} l\right)\right]}{\left(k + \frac{\omega}{\omega_{\sigma}} l\right) \sinh(2\pi^2 l/\beta\hbar\omega_{\sigma})} \right], \quad (2.10) \end{aligned}$$

where  $\omega_{\pm} = (\omega \pm \omega_c)/2$  and the relation  $\mu \gg T$  is assumed. In the derivation of oscillatory terms in  $\Omega_{osc}$ , we used the approximation as follows,

$$\begin{aligned} & \int_{-\beta(\mu-\eta)}^{\infty} d\xi \frac{e^{\xi}}{(e^{\xi} + 1)^2} \cdot e^{i\frac{2\pi k}{\beta\hbar\omega}\xi} \\ & \simeq \int_{-\infty}^{\infty} d\xi \frac{e^{\xi}}{(e^{\xi} + 1)^2} \cdot e^{i\frac{2\pi k}{\beta\hbar\omega}\xi} \cdot \theta[\mu - \eta], \quad (2.11) \end{aligned}$$

where  $\theta[x]$  is the Heaviside function.

As is known from eq. (2.8),  $\Omega_0$  is dependent on a magnetic field only through the chemical potential  $\mu(H, T)$ , which is regarded as a function of the field and temperature and almost a constant as a function of the field when  $\mu/\hbar\omega_c \gg 1$ . Therefore the contribution of  $\Omega_0$  to the magnetic moment is much smaller than those due to  $\Omega_L$  and  $\Omega_{osc}$ .

Based on this result, the field dependence of the magnetic moment is classified into three regions; “Mesoscopic Fluctuation (MF)”, “Landau Diamagnetism (LD)” and “de Haas-van Alphen (dHvA)”, as is shown in Fig. 1. “MF” corresponds to the region as  $T \lesssim \hbar\omega_-$ , which implies  $T/\hbar\omega_0 \lesssim 1$  under a weak field ( $\omega_c/\omega_0 \lesssim 1$ ) and  $T/\hbar\omega_0 \lesssim (\omega_c/\omega_0)^{-1}$  under a strong field ( $\omega_c/\omega_0 \gtrsim 1$ ), while “LD” corresponds to the region as  $T \gtrsim \hbar\omega_+$ , which requires  $T/\hbar\omega_0 \gtrsim 1$  under a weak field ( $\omega_c/\omega_0 \lesssim 1$ ) and  $T/\hbar\omega_0 \gtrsim \omega_c/\omega_0$  under a strong field ( $\omega_c/\omega_0 \gtrsim 1$ ). The other region in Fig. 1 is “dHvA”.

Fig. 2 shows field dependences of magnetic moment at various temperatures; (a),(b) and (c),(d) are respectively under a weak field ( $\omega_c \lesssim \omega_0$ ) and a strong field ( $\omega_c \gtrsim \omega_0$ ).  $N_0$  is set at 5000 in this calculation. At first, we focus on the region of a weak field ( $\omega_c \lesssim \omega_0$ ) shown in (a) and (b), where (a) corresponds to “MF” and (b) ranges from “MF” to “LD”. At low temperature as  $T \lesssim \hbar\omega_0$  corresponding to “MF”, the magnetic moment shows a large fluctuation with respect to the field, as Yoshioka and Fukuyama have shown. In this “MF” region, all the oscillatory terms in  $\Omega_{osc}$  contribute to the magnetic moment leading to such a large fluctuation, in addition

to  $\Omega_L = -1/2 \cdot \chi_L H^2$  ( $\chi_L = -1/3 \cdot D_0 \mu_B^2$ , the Landau diamagnetic susceptibility, where  $D_0 = \mu/(\hbar\omega_0)^2$ , the density of states at Fermi energy), which leads to the usual Landau diamagnetism. Particularly at much lower temperature ( $T \ll \hbar\omega_0$ ) and under a much weaker field ( $\omega_c \ll \omega_0$ ), the magnetic moment shows a strong paramagnetism, which was first noticed by Meier and Wyder<sup>8)</sup> and discussed by Budzin et al.<sup>9)</sup> This strong paramagnetism is attributed to the rotational symmetry of the system. Hence, in the presence of weak disorder, a large spatial variation of magnetic moment, either paramagnetic or diamagnetic, is expected, which fact is the cause of a large variance of orbital susceptibility in the limit of weak magnetic field at low temperature.<sup>16,17,18,19,20)</sup> As the temperature is raised ( $T \gtrsim \hbar\omega_0$ ) under such a weak field ( $\omega_c \lesssim \omega_0$ ), the fluctuation of magnetic moment is reduced and the magnetic moment becomes linearly dependent on the field, the slope of which gives the Landau diamagnetic susceptibilities  $\chi_L$  corresponding to “LD”. In this “LD” region, the contribution of  $\Omega_{osc}$  are reduced and  $\Omega_L$  becomes dominant.

Fig. 2(c) and (d) show the field dependence of magnetic moment under a strong field ( $\omega_c \gtrsim \omega_0$ ) at various temperatures. (c) and (d) range from “MF” to “dHvA” and from “dHvA” to “LD”, respectively. At low temperature as  $T \lesssim \hbar\omega_- \simeq \hbar\omega_0^2/\omega_c$ , magnetic moment shows slow oscillation with a large amplitude and rapid oscillation with a small amplitude, as is shown in Fig. 2(c). The former oscillation with respect to the field is characterized by  $\mu/\hbar\omega \simeq \mu/\hbar\omega_c$ , which is caused by the periodic intersections of chemical potential  $\mu$  by the Landau level (the states characterized by  $n$  in eq. (2.4)) and corresponds to the de Haas-van Alphen oscillation. The latter oscillation with respect to the field is governed by  $\phi/\phi_0$  where  $\phi$  is the total flux penetrating the system and  $\phi_0 = hc/e$ , flux quantum. When the total magnetic flux is increased by  $\phi_0$ , the degeneracy of each Landau level under Fermi energy is increased by unity. This causes the oscillation of the magnetic moment with a period  $\phi_0$  as a function of  $\phi$  at such a low temperature as  $T \lesssim \hbar\omega_- \simeq \hbar\omega_0^2/\omega_c$  which is energy spacing between different angular momentum states at each Landau level. Physically, this oscillation is caused by a coherent motion of electrons along the edge and can be considered as the Aharonov-Bohm oscillation. Such a behavior under a strong field ( $\omega_c \gtrsim \omega_0$ ) has been noted at  $T = 0$  by Meir, Wohlman, and Gefen.<sup>13)</sup> As the temperature is raised so as  $\hbar\omega_- \lesssim T \lesssim \hbar\omega_+ \simeq \hbar\omega_c$  under such a strong field ( $\omega_c \gtrsim \omega_0$ ) corresponding to “dHvA”, the AB oscillation disappears and there only remains the dHvA oscillation. In this “dHvA” region, the first term in  $\Omega_{osc}$  has an appreciable contribution in addition to  $\Omega_L$ . At much higher temperature ( $T \gtrsim \hbar\omega_+ \simeq \hbar\omega_c$ ), the dHvA oscillation disappears and magnetic moment shows a linear field dependence, i.e. the Landau diamagnetism as seen in Fig. 2(d) e.g.  $T/\hbar\omega_0 = 4$ .

### §3. Spatial Distribution of Current and Magnetic Moment

In this section, we study the relationship between a spatial distribution of current and a magnetic moment of the whole system, the latter of which is given by the thermodynamic potential  $\Omega$  in the previous section.

The spatial distribution of current in the system is given as follows,

$$\begin{aligned}\mathbf{J}(\mathbf{r}) &= \text{Re} \left\langle \hat{\psi}^\dagger(\mathbf{r}) \frac{(-e)}{m} \left( \hat{\mathbf{p}}(\mathbf{r}) + \frac{e}{c} \mathbf{A}(\mathbf{r}) \right) \hat{\psi}(\mathbf{r}) \right\rangle \\ &= J_\theta(r) \mathbf{e}_\theta,\end{aligned}\tag{3.1}$$

where  $\langle \dots \rangle$  denotes the thermal average and  $\hat{\psi}(\mathbf{r})$  is the field operator and  $\mathbf{e}_\theta = \frac{\partial \mathbf{r}}{\partial \theta} / \left| \frac{\partial \mathbf{r}}{\partial \theta} \right|$  as shown in Fig. 3. By use of the eigenstates in eq. (2.3) as the basis,  $J_\theta(r)$  is given as

$$J_\theta(r) = (-e)v_0 \sum_{n\alpha} \left[ \alpha \left( \frac{r}{\xi} \right)^{-1} + \frac{\omega_c}{2\omega_0} \left( \frac{r}{\xi} \right) \right] R_{n\alpha}(r)^2 f(E_{n\alpha}),\tag{3.2}$$

where  $\xi = \sqrt{\hbar/m\omega_0}$ , the characteristic length, and  $v_0 = \omega_0 \xi$ , the characteristic velocity of electrons.

This local current  $\mathbf{J}(\mathbf{r})$  induces a magnetic moment  $\mathbf{M}(\mathbf{r})$  given as follows,

$$\begin{aligned}\mathbf{M}(\mathbf{r}) &= \frac{1}{2c} \mathbf{r} \times \mathbf{J}(\mathbf{r}) \\ &= \frac{1}{2c} r J_\theta(r) \mathbf{e}_z \\ &\equiv M_z(r) \mathbf{e}_z.\end{aligned}\tag{3.3}$$

Therefore, by integrating this magnetic moment with respect to  $\mathbf{r}$ , we get the relation between the total magnetic moment  $M$  ( $z$ -component) and the local current  $J_\theta(r)$  as

$$\begin{aligned}M &= \int dS M_z(r) \\ &= \frac{\pi}{c} \int_0^\infty dr r^2 J_\theta(r).\end{aligned}\tag{3.4}$$

This expression of magnetic moment derived from the local current density coincides with the one in eq. (2.6) derived from the thermodynamic potential (see Appendix B).

### 3.1 Region of Weak Magnetic Field ( $\omega_c \lesssim \omega_0$ )

Here, we focus on the properties of the spatial distribution of current in the weak field region ( $\omega_c \lesssim \omega_0$ ). At low temperature ( $T \lesssim \hbar\omega_0$ , i.e. in ‘‘MF’’), the magnetic moment shows a large fluctuation as a function of the field. The spatial distribution of current in such a situation is shown in Fig. 4(a), which indicates that  $J_\theta(r)$  can be either positive or negative, i.e. paramagnetic or diamagnetic, respectively. In the bulk region (mainly,  $r \lesssim R$ ), large currents flow paramagnetically or diamagnetically depending on  $r$ . This large bulk currents are sensitive to the strength of the field and lead to the large fluctuation of magnetic moment. This behavior of  $J_\theta(r)$  is a characteristic feature of local currents in the region of ‘‘MF’’.

As the temperature is raised ( $T \gtrsim \hbar\omega_0$ ) under such a weak field, the fluctuation of magnetic moment disappears and the magnetic moment shows the Landau diamagnetism as discussed in

the previous section. According with this change of magnetic moment, the spatial distribution of current  $J_\theta(r)$  is changed as shown in Fig. 4(b); the fluctuating large bulk currents are immediately reduced and finally the diamagnetic current flowing along the edge ( $r \simeq R$ ) only survives. It is seen that this property of the current distribution in “LD” is characteristic of two-dimensional confined system as deduced from the Kubo’s formula of the current distribution, which will be explained in the following.

Based on the Wigner representation, Kubo<sup>4)</sup> derived the analytic form of a current distribution proportional to a magnetic field and leading to the Landau diamagnetism in the system under a confining potential  $V(r)$ , which is assumed to be slowly varying in space compared to the electron wave length. The expansion parameters in this theory are  $\hbar^2 e H \frac{dV(r)}{dr} / m^{3/2} c T^{5/2}$ ,  $(\hbar e H / m c T)^2$ ,  $\hbar^2 \left( \frac{dV(r)}{dr} \right)^2 / m T^3$  and  $\hbar^2 \frac{d^2 V(r)}{dr^2} / m T^2$ . In the present model of harmonic confining potential, the parameters are explicitly given as  $\omega_c / \omega_0 \cdot (T / \hbar \omega_0)^{-5/2} \cdot R / \xi$ ,  $(\omega_c / \omega_0)^2 \cdot (T / \hbar \omega_0)^{-2}$ ,  $(T / \hbar \omega_0)^{-3} \cdot (R / \xi)^2$  and  $(T / \hbar \omega_0)^{-2}$  respectively, by replacing  $r$  with the system radius  $R$ . After all,  $T / \hbar \omega_0 \gtrsim (R / \xi)^{2/3}$  and  $T / \hbar \omega_0 \gtrsim \omega_c / \omega_0$  are required for the validity of the expansion in the Wigner representation, which are actually a part of the region “LD” in Fig. 1 ( However, such an expansion turns out to be an asymptotic one since our analytic result shows that  $\hbar = 0$  is an essential singularity. See Appendix C for a detail. ). The spatial distribution of current, which is valid under such a condition, is given as follows in general,

$$\mathbf{J}(\mathbf{r}) = \frac{1}{3} c \mu_B^2 \mathbf{H} \times \nabla n(\mathbf{r}), \quad (3.5)$$

where

$$n(\mathbf{r}) = \frac{1}{h^d} \int d\boldsymbol{\pi} \int dE \delta' \left( E - \frac{\boldsymbol{\pi}^2}{2m} - V(\mathbf{r}) \right) f(E), \quad (3.6)$$

$d$  is the dimension of the system and  $\boldsymbol{\pi}$  corresponds to a physical momentum. The magnetic moment due to this current density becomes  $\chi_L H$ , the Landau diamagnetism.

In the present two-dimensional system,  $\boldsymbol{\pi}$  and  $E$ -integration in eq. (3.6) can be easily performed and  $n(\mathbf{r})$  is given by

$$n(\mathbf{r}) = \frac{2\pi m}{\hbar^2} f(V(\mathbf{r})), \quad (3.7)$$

and  $\mathbf{J}(\mathbf{r})$  becomes

$$\mathbf{J}(\mathbf{r}) = \frac{1}{3} c \mu_B^2 \cdot \frac{2\pi m}{\hbar^2} \cdot \mathbf{H} \times \nabla V(\mathbf{r}) \cdot f'(V(\mathbf{r})). \quad (3.8)$$

Due to the factor  $f'(V(\mathbf{r}))$  which reflects Fermi degeneracy, this form of a current distribution means that the diamagnetic current flows only in the region  $V(\mathbf{r}) \simeq \mu$ , i.e. the edge of the system, even if the potential is varying spatially in the bulk region.

Applying the above formula to the present model  $V(r) = m\omega_0^2 r^2 / 2$ , we get  $\mathbf{J}(\mathbf{r})$  as

$$\mathbf{J}(\mathbf{r}) = -\frac{j_0}{6} \cdot \frac{\omega_c}{\omega_0} \cdot \left( \frac{T}{\hbar \omega_0} \right)^{-1} \cdot \frac{r}{\xi} \cdot \frac{e^{\beta(V(r)-\mu)}}{(e^{\beta(V(r)-\mu)} + 1)^2} \cdot \mathbf{e}_\theta, \quad (3.9)$$

where

$$\beta(V(r) - \mu) = \frac{1}{2} \cdot \left( \frac{T}{\hbar\omega_0} \right)^{-1} \left[ \left( \frac{r}{\xi} \right)^2 - \left( \frac{R}{\xi} \right)^2 \right], \quad (3.10)$$

and  $j_0 = e\omega_0/4\pi\xi$  the characteristic current density. The current distribution calculated by eq. (3.9) coincides with the one obtained from eq. (3.2). ( For example, at  $\omega_c/\omega_0 = 0.1$  and  $T/\hbar\omega_0 = 10$ , the agreement is within 0.5% numerically.)

In comparison, the case of  $d = 3$  which Kubo considered appears somewhat different, since the current both at the surface region ( the region as  $V(\mathbf{r}) \simeq \mu$  ) and the bulk region can contribute to the magnetic moment. To see this, we approximate a Fermi distribution function in eq. (3.6) by the linearized form around the Fermi energy as

$$f(E) \simeq \begin{cases} 1 & ( E < \mu - 2T ) \\ \frac{1}{2} - \frac{E-\mu}{4T} & ( |E - \mu| \leq 2T ) \\ 0 & ( E > \mu + 2T ) \end{cases} . \quad (3.11)$$

We assume the confining potential  $V(\mathbf{r})$  is only dependent on  $r$  in cylindrical coordinates  $(r, \theta, z)$ . Then the current distribution is given by

$$\mathbf{J}(\mathbf{r}) = -\frac{\gamma H}{\sqrt{T}} \cdot V'(r) \cdot g(V(r)) \mathbf{e}_\theta, \quad (3.12)$$

where  $\gamma = \sqrt{2}\pi m^{3/2} c \mu_B^2 / 3h^3$  and  $g(V(r))$ , the function corresponding to  $f'(V(r))$  in the case of  $d = 2$  is given as

$$g(V(r)) = \begin{cases} \sqrt{\frac{\mu-V(r)}{T} + 2} - \sqrt{\frac{\mu-V(r)}{T} - 2} & ( V(r) < \mu - 2T ) \\ \sqrt{\frac{\mu-V(r)}{T} + 2} & ( |V(r) - \mu| \leq 2T ) \\ 0 & ( V(r) > \mu + 2T ) \end{cases} . \quad (3.13)$$

In the bulk region where  $V(r) \ll \mu - 2T$ ,  $g(V(r))$  becomes

$$g(V(r)) \simeq \frac{2}{\sqrt{\frac{\mu-V(r)}{T}}} \ll 1 , \quad (3.14)$$

while at the surface region,  $|V(r) - \mu| < 2T$ ,  $g(V(r)) \sim 1$ . Therefore, it can be said that the current causing the Landau diamagnetism is mainly induced at the surface also in a three-dimensional system, which is not so clear as the case of  $d = 2$ .

At low temperature as  $T \lesssim \hbar\omega_0$ , on the other hand, the contributions of higher order terms in magnetic field become larger and the above formula of current density is not valid. Then, the current distribution changes dramatically at around the temperature  $T = \hbar\omega_0$  under a weak field ( $\omega_c \lesssim \omega_0$ ) as is shown in Fig. 4(a) and (b) and this change is clearly reflected in a magnetic moment of the system. Hajdu and Shapiro<sup>15)</sup> studied a two-dimensional system under a confining potential  $V(\mathbf{r}) = m\omega_0^2 x^2/2$  ( i.e. harmonic groove ) with a width  $L_x$  and an arbitrary long length  $L_y$  by



imposing a periodic boundary condition in the  $y$ -direction, and pointed out that the temperature as  $T = \hbar\omega_0$  below which magnetic moment shows a large fluctuation under a weak field ( $\omega_c \lesssim \omega_0$ ) corresponds to  $\hbar/\tau_{tr}$  where  $\tau_{tr} = L_x/v_F$ , time of propagation for electrons at the Fermi energy across the groove. The physical reason why the field dependence of magnetic moment shows such a dramatic difference depending on the temperature is understood as follow. When the effect of a confining potential  $V(\mathbf{r})$  is considered perturbative, the thermal Green's function of a degenerate electrons has the following damping factor,

$$G(x, \tau = 0) \propto e^{-\frac{\pi T}{\hbar v_F} x}. \quad (3.15)$$

Therefore, the length  $\hbar v_F/\pi T \equiv l_c$  is regarded as the coherence length of degenerate electrons. Under the condition  $l_c \gtrsim L$ , where  $L$  is a system length, electrons near the Fermi surface can propagate from one side of the system to the other side with a small damping and experience the multiple reflection by the boundary potential as shown in Fig. 5(a). Therefore electrons near the Fermi surface, which play an essential role in the orbital magnetism of degenerate electron system, are strongly affected by the boundary potential. In this model, the condition  $l_c \gtrsim L$  corresponds to  $T \lesssim \hbar\omega_0$  i.e. ‘‘MF’’. As shown in Fig. 4 (a), it is seen that this multiple reflection induces large currents irregularly distributed paramagnetically or diamagnetically in the bulk region, which are sensitive to the strength of a magnetic field and causes the large fluctuation of a magnetic moment as a function of the field. On the other hand, under the condition  $l_c \lesssim L$  ( $T \gtrsim \hbar\omega_0$ ), the effect of the multiple reflection by the boundary potential wall is reduced as shown in Fig. 5(b), and this is considered to lead to the suppression of the bulk currents and the recovery of the Landau diamagnetism. Considering the case of a harmonic groove system based on this idea, which Hajdu and Shapiro<sup>15)</sup> studied, it is natural that the relative magnitude of  $l_c$  and the width  $L_x$  affects the field dependence of magnetic moment while  $L_y$  does not affect it qualitatively, since the  $x$ -direction is actually confined by a harmonic potential and a multiple reflection can happen only in the  $x$ -direction.

Robnik<sup>10)</sup> discussed the size effect on the zero-field susceptibility in a system confined by a hard wall, based on the Green's function method, and concluded that at  $T = 0$  the contribution of the boundary wall to the susceptibility is always paramagnetic but with the order of magnitude  $(k_F L)^{-1}$  compared to the Landau susceptibility, where  $k_F$  is a Fermi wave number and  $L$  is a system length. As is clear from Fig. 2(a), this evaluation of a size effect due to the confining potential is too small. This disagreement can be attributed to the fact that the multiple reflection by the boundary potential wall is disregarded in ref. 9.

### 3.2 Region of Strong Magnetic Field ( $\omega_c \gtrsim \omega_0$ )

Under a strong magnetic field ( $\omega_c \gtrsim \omega_0$ ), the energy spectrum in eq. (2.4) becomes close to the one without the confining potential, i.e. the Landau level ( the states characterized by  $n$  in eq. (2.4)

). At low temperature as  $T \lesssim \hbar\omega_c$ , magnetic moment is affected by this Landau quantization and oscillates as a function of the field as is shown in Fig. 2(c) and (d) (This is the familiar de Haas-van Alphen effect). In this “dHvA”, the spatial distribution of current is as is shown in Fig. 4(c). Several diamagnetic peaks can be seen and paramagnetic currents flow between them. These bulk currents are much larger than the edge current in “LD”, although the diamagnetic currents are almost cancelled by the paramagnetic ones as an average. Each diamagnetic peak comes from the state with the same  $n$  in eq. (2.4) which corresponds to Landau level. In this model, each Landau level has a different degeneracy with respect to the angular momentum,  $\alpha$ , due to the confining potential and the lower Landau level has the higher degeneracy. Therefore, the spatial extent of the lower Landau level with such a degeneracy becomes larger and is reflected in the current distribution as the spatially separated diamagnetic peaks. As the field is raised, the number of Landau level below the Fermi energy decreases and the diamagnetic peaks closest to the center of the system disappear one by one. This change of the current distribution causes the large oscillation of the magnetic moment as a function of the field. At much lower temperature in “MF” ( $T \lesssim \hbar\omega_-$ ) where the AB effect appears, the current distribution is almost same as in “dHvA” region.

At higher temperature as  $T \gtrsim \hbar\omega_c$ , the diamagnetic peaks in the bulk region are smeared out and there remain only edge current as is shown in Fig. 4(d). This edge current is spatially broadened compared to the one at lower temperature in “LD” shown in Fig. 4(b). This temperature dependence of edge current is understood from eq. (3.9) where the spatial extent of edge current corresponds to  $|V(r) - \mu| \lesssim T$ .

#### §4. Summary

We have studied the relation between the spatial distribution of current and the magnetic moment of the whole system in a two-dimensional electron system under an isotropic harmonic potential as  $V(\mathbf{r}) = m\omega_0^2 r^2/2$ . It is found that characteristic dependences of magnetic moment on temperature and magnetic field are clearly reflected in the spatial distribution of current.

Under a weak field ( $\omega_c \lesssim \omega_0$ ), the field dependence of magnetic moment dramatically changes at around the temperature  $T = \hbar\omega_0$ . In the low temperature region ( $T \lesssim \hbar\omega_0$ ), magnetic moment shows a large fluctuation as a function of the field, as was indicated by Yoshioka and Fukuyama.<sup>14)</sup> We attribute this large fluctuation of magnetic moment to a multiple reflection by the boundary confining potential, which becomes important once the coherence length of degenerate electrons  $l_c = \hbar v_F/\pi T$  gets longer than a system length. In the present model, the system length is characterized by the radius  $R$  and the above condition leads to  $l_c \gtrsim R$  implying  $T \lesssim \hbar\omega_0$ . At such low temperature, it is seen that the multiple reflection induces large currents irregularly distributed paramagnetically or diamagnetically in the bulk region, which are sensitive to the strength of the field and cause a large fluctuation of the magnetic moment. As the temperature

is raised ( $T \gtrsim \hbar\omega_0$ ), the fluctuations of the magnetic moment are reduced and the usual Landau diamagnetism is recovered. Corresponding to this change, it is found that the large currents in the bulk region are immediately reduced and finally the diamagnetic current flowing along the edge (in the region satisfying  $V(\mathbf{r}) \simeq \mu$ ) only survives, which leads to the Landau diamagnetism. This edge current is regarded characteristic of a two-dimensional confined system, as inferred from the Kubo<sup>4)</sup>'s formula of the diamagnetic current distribution which is derived for high temperature as  $T \gtrsim \hbar\omega_0 \cdot (R/\xi)^{2/3}$  and  $\hbar\omega_c$ , where  $\xi = \sqrt{\hbar/m\omega_0}$ , the characteristic length. From this formula, the cancellation of the bulk currents is seen to be due to the Fermi degeneracy. It is also noted that the persistence of the diamagnetic current at the surface is also seen in a three-dimensional system.

Under a strong field ( $\omega_c \gtrsim \omega_0$ ), dHvA effect appears at low temperature as  $T \lesssim \hbar\omega_c$ . In this situation, the current is distributed in the bulk region and diamagnetic peaks appear, although paramagnetic currents flow between the peaks, which almost cancel the contribution of the diamagnetic peaks as an average. Here, each peak is due to the Landau level with different degeneracy because of the confining potential. As the field is increased, this diamagnetic peak disappears one by one corresponding to the decrease of the number of Landau levels under the Fermi energy, and this causes the large oscillation of magnetic moment (dHvA effect). At much lower temperature ( $T \lesssim \hbar\omega_- \simeq \hbar\omega_0^2/\omega_c$ , the energy spacing between different angular momentum states at each Landau level), the small but rapid oscillation with a period  $\phi_0 = hc/e$  appears as a function of the total flux  $\phi$  in addition to the dHvA oscillation, which was originally found by Meir et al<sup>13)</sup> at  $T = 0$ . This oscillation is caused by a coherent motion of electrons along the edge and can be called AB oscillation. On the other hand, at high temperature as  $T \gtrsim \hbar\omega_c$  under such a strong field, the bulk currents are quickly reduced and the Landau diamagnetism by the edge current is recovered as in the case under a weak field. It should be noticed that this edge current does not cause AB oscillations, because the current is due to incoherent motions of electrons.

## Acknowledgment

One of the authors (Y. I) would like to express his sincerest gratitude to Hiroshi Kohno for stimulating and instructive discussions and thank Masakazu Murakami for instructive and useful discussions.

## Appendix A: Derivation of Magnetic Moment from Thermodynamical Potential $\Omega$

The thermodynamic potential  $\Omega$  is given by

$$\Omega = -\frac{1}{\beta} \sum_{n=0}^{\infty} \sum_{\alpha=-\infty}^{\infty} \log \left[ 1 + e^{-\beta(E_{n\alpha} - \mu)} \right], \quad (\text{A}\cdot 1)$$

where  $E_{n\alpha} = \hbar\omega(n + 1/2) + \hbar\omega|\alpha|/2 + \hbar\omega_c \alpha/2$ .

By applying the Poisson summation formula

$$\sum_{n=0}^{\infty} F\left(n + \frac{1}{2}\right) = \int_0^{\infty} dx F(x) + 2 \operatorname{Re} \sum_{k=1}^{\infty} (-1)^k \int_0^{\infty} dx F(x) e^{2\pi i k x}, \quad (\text{A}\cdot 2)$$

to the sum over  $n$ ,  $\Omega$  is transformed as

$$\begin{aligned} \Omega = & -\frac{1}{\beta\hbar\omega} \int_0^{\infty} d\varepsilon \left[ 1 + 2 \operatorname{Re} \sum_{k=1}^{\infty} (-1)^k e^{2\pi i k \frac{\varepsilon}{\hbar\omega}} \right] \log \left[ 1 + e^{-\beta(\varepsilon-\mu)} \right] \\ & - \frac{1}{\beta\hbar\omega} \int_0^{\infty} d\varepsilon \left[ 1 + 2 \operatorname{Re} \sum_{k=1}^{\infty} (-1)^k e^{2\pi i k \frac{\varepsilon}{\hbar\omega}} \right] \sum_{\sigma=\pm} \sum_{\alpha=1}^{\infty} \log \left[ 1 + e^{-\beta(\hbar\omega_{\sigma}\alpha + \varepsilon - \mu)} \right], \end{aligned} \quad (\text{A}\cdot 3)$$

where  $\omega_{\pm} = (\omega \pm \omega_c)/2$ .

To the sum over  $\alpha$ , we again use the Poisson summation formula as

$$\frac{1}{2} F(0) + \sum_{\alpha=1}^{\infty} F(\alpha) = \int_0^{\infty} dx F(x) + 2 \operatorname{Re} \sum_{l=1}^{\infty} \int_0^{\infty} dx F(x) e^{2\pi i l x}. \quad (\text{A}\cdot 4)$$

Then  $\Omega$  is given as

$$\begin{aligned} \Omega = & -\frac{1}{\beta(\hbar\omega_0)^2} \int_0^{\infty} d\varepsilon \int_0^{\infty} d\eta \left[ 1 + 2 \operatorname{Re} \sum_{k=1}^{\infty} (-1)^k e^{2\pi i k \frac{\varepsilon}{\hbar\omega}} \right] \cdot \log \left[ 1 + e^{-\beta(\varepsilon+\eta-\mu)} \right] \\ & - \sum_{\sigma=\pm} \frac{2}{\beta\hbar\omega \cdot \hbar\omega_{\sigma}} \operatorname{Re} \sum_{l=1}^{\infty} \int_0^{\infty} d\varepsilon \int_0^{\infty} d\eta \log \left[ 1 + e^{-\beta(\varepsilon+\eta-\mu)} \right] \cdot e^{2\pi i l \frac{\eta}{\hbar\omega_{\sigma}}} \\ & - \sum_{\sigma=\pm} \frac{4}{\beta\hbar\omega \cdot \hbar\omega_{\sigma}} \operatorname{Re} \sum_{k=1}^{\infty} (-1)^k \int_0^{\infty} d\varepsilon e^{2\pi i k \frac{\varepsilon}{\hbar\omega}} \cdot \operatorname{Re} \sum_{l=1}^{\infty} \int_0^{\infty} d\eta \log \left[ 1 + e^{-\beta(\varepsilon+\eta-\mu)} \right] \cdot e^{2\pi i l \frac{\eta}{\hbar\omega_{\sigma}}}. \end{aligned} \quad (\text{A}\cdot 5)$$

We perform integrations over  $\varepsilon$  and  $\eta$  twice by parts,

$$\begin{aligned} & \int_0^{\infty} d\varepsilon \log \left[ 1 + e^{-\beta(\varepsilon+\eta-\mu)} \right] \cdot e^{2\pi i k \frac{\varepsilon}{\hbar\omega}} \\ = & -\frac{\hbar\omega}{2\pi i k} \log \left[ 1 + e^{-\beta(\eta-\mu)} \right] + \beta \left( \frac{\hbar\omega}{2\pi k} \right)^2 f(\eta) \\ & - \beta \left( \frac{\hbar\omega}{2\pi k} \right)^2 e^{2\pi i k \frac{\mu-\eta}{\hbar\omega}} \int_{-\beta(\mu-\eta)}^{\infty} d\xi \frac{e^{\xi}}{(e^{\xi} + 1)^2} \cdot e^{i \frac{2\pi k}{\beta\hbar\omega} \xi}. \end{aligned} \quad (\text{A}\cdot 6)$$

In the last integration term, we assume  $\mu \gg T$  and approximate as

$$\begin{aligned} & \int_{-\beta(\mu-\eta)}^{\infty} d\xi \frac{e^{\xi}}{(e^{\xi} + 1)^2} \cdot e^{i \frac{2\pi k}{\beta\hbar\omega} \xi} \\ \simeq & \int_{-\infty}^{\infty} d\xi \frac{e^{\xi}}{(e^{\xi} + 1)^2} \cdot e^{i \frac{2\pi k}{\beta\hbar\omega} \xi} \cdot \theta[\mu - \eta] \\ = & \frac{\frac{2\pi^2 k}{\beta\hbar\omega}}{\sinh\left(\frac{2\pi^2 k}{\beta\hbar\omega}\right)} \cdot \theta[\mu - \eta], \end{aligned} \quad (\text{A}\cdot 7)$$

where  $\theta[x]$  is the Heaviside function.

By using this approximation and the relations

$$\sum_{k=1}^{\infty} \frac{(-1)^{k+1}}{k^2} = \frac{\pi^2}{12}, \quad \sum_{k=1}^{\infty} \frac{1}{k^2} = \frac{\pi^2}{6}, \quad (\text{A}\cdot 8)$$

we get the form represented in eq. (2.7).

## Appendix B: Derivation of Magnetic Moment from Current Distribution

By replacing  $r^2/2l^2$  in eq. (3.4) with  $\rho$ , magnetic moment is given by

$$M = -\mu_B \sum_{n=0}^{\infty} \sum_{\alpha=-\infty}^{\infty} \frac{n!}{(n+|\alpha|)!} f(E_{n\alpha}) \cdot \int_0^{\infty} d\rho \left[ \alpha + \frac{\omega_c}{\omega} \rho \right] e^{-\rho} \rho^{|\alpha|} L_n^{(|\alpha|)}[\rho]^2. \quad (\text{B}\cdot 1)$$

$\rho$ -integrations can be performed as

$$\int_0^{\infty} d\rho e^{-\rho} \rho^{|\alpha|} L_n^{(|\alpha|)}[\rho] L_m^{(|\alpha|)}[\rho] = \frac{(n+|\alpha|)!}{n!} \delta_{nm}, \quad (\text{B}\cdot 2)$$

and

$$\begin{aligned} & \int_0^{\infty} d\rho e^{-\rho} \rho^{|\alpha|+1} L_n^{(|\alpha|)}[\rho]^2 \\ &= \int_0^{\infty} d\rho e^{-\rho} \rho^{|\alpha|+1} \left[ L_n^{(|\alpha|+1)}[\rho] - L_{n-1}^{(|\alpha|+1)}[\rho] \right]^2 \\ &= \frac{(n+|\alpha|+1)!}{n!} + \frac{(n+|\alpha|)!}{(n-1)!} \\ &= \frac{(n+|\alpha|)!}{n!} \cdot (2n+|\alpha|+1). \end{aligned} \quad (\text{B}\cdot 3)$$

Therefore, the magnetic moment becomes

$$\begin{aligned} M &= -\mu_B \sum_{n=0}^{\infty} \sum_{\alpha=-\infty}^{\infty} \left[ \alpha + \frac{\omega_c}{\omega} \cdot (2n+|\alpha|+1) \right] f(E_{n\alpha}) \\ &= \sum_{n\alpha} \left( -\frac{\partial E_{n\alpha}}{\partial H} \right) f(E_{n\alpha}). \end{aligned} \quad (\text{B}\cdot 4)$$

This coincides with the one derived from the thermodynamical potential in eq. (2.6).

## Appendix C: Wigner Representation for Landau Diamagnetism

In the present model of the harmonic confining potential, the parameter region, where the Kubo's formula of current distribution leading to the Landau diamagnetism<sup>4)</sup> is valid, is  $T/\hbar\omega_0 > \sim (R/\xi)^{2/3} = (2 \cdot \mu/\hbar\omega_0)^{1/3}$  and  $T/\hbar\omega_0 \gtrsim \omega_c/\omega_0$ , which is dependent on the chemical potential,  $\mu$ , i.e. the number of electrons. This region is only a small part of "LD" region ( $T/\hbar\omega_0 \gtrsim 1$  and  $T/\hbar\omega_0 \gtrsim \omega_c/\omega_0$ ) of Fig. 1. The reason of this apparent discrepancy is as follows.

By differentiating the trigonometric functions in eq. (2.10) with respect to the field, it is found that  $\Omega_{osc}$  contributes to the magnetic moment in the order of magnitude  $(2\pi^2 T/\hbar\omega)/\sinh(2\pi^2 T/\hbar\omega)$  or

$(2\pi^2 T/\hbar\omega_{\pm})/\sinh(2\pi^2 T/\hbar\omega_{\pm})$  relative to  $\Omega_L$ , and based on this fact the phase diagram in Fig. 1 is decided. These factors  $(2\pi^2 T/\hbar\omega)/\sinh(2\pi^2 T/\hbar\omega)$  and  $(2\pi^2 T/\hbar\omega_{\pm})/\sinh(2\pi^2 T/\hbar\omega_{\pm})$  can not be expanded in terms of  $\hbar\omega/T$  and  $\hbar\omega_{\pm}/T$ , which are seen to correspond to the expansion parameters in the treatment of Wigner representation. This implies that one cannot conclude whether the bulk magnetic moment shows the Landau diamagnetism or not, unless the contributions of higher order terms in  $\hbar$  in Wigner representation are summed up to the infinite order. Actually, in the parameter region,  $1 \lesssim T/\hbar\omega_0 \lesssim (R/\xi)^{2/3}$  and  $T/\hbar\omega_0 \gtrsim \omega_c/\omega_0$ , some expansion parameters in ref. 4 get larger than 1, but even in such a case, the Landau diamagnetism is realized and diamagnetic current is mainly induced at the edge as seen in Fig. 4(b).

- 
- [1] N. Bohr: Ph.D. thesis, Univ. of Copenhagen (1911)
  - [2] J. H. van Vleck: *The Theory of Electric and Magnetic Susceptibilities* (Clarendon Press, Oxford, 1932) §26, 81.
  - [3] L. D. Landau: Z. Phys. **64** (1930) 629.
  - [4] R. Kubo: J. Phys. Soc. Jpn. **19** (1964) 2127.
  - [5] L. Friedman: Phys. Rev. **134** (1964) A336.
  - [6] D. Childers and P. Pincus: Phys. Rev. **177** (1969) 1036.
  - [7] R. V. Denton: Z. Phys. **265** (1973) 119.
  - [8] F. Meir and P. Wyder: Phys. Rev. Lett. **30** (1973) 181.
  - [9] A. I. Buzdin, O. V. Dolgov and Yu. E. Lozovik: Phys. Lett. **100A** (1984) 261.
  - [10] M. Robnik: J. Phys. A: Gen. Phys. **19** (1986) 3619.
  - [11] R. Nemeth: Z. Phys. B **81** (1990) 89.
  - [12] J. M. van Ruitenbeek and D. A. van Leeuwen: Phys. Rev. Lett. **67** (1991) 640.
  - [13] Y. Meir, O. Entin-Wohlmann and Y. Gefen: Phys. Rev. B **42** (1990) 8351.
  - [14] D. Yoshioka and H. Fukuyama: J. Phys. Soc. Jpn. **61** (1992) 2368.
  - [15] J. Hajdu and B. Shapiro: Europhys. Lett **28** (1994) 61.
  - [16] O. D. Cheishvili: Pis'ma Zh. Eksp. Theor. Fiz. **48** (1988) 206. translation: JETP Lett. **48** (1988) 225.
  - [17] H. Fukuyama: J. Phys. Soc. Jpn. **58** (1989) 47.
  - [18] R. A. Serota and S. Oh: Phys. Rev. B **41** (1990) 10523.
  - [19] S. Oh, A. Yu. Zyuzin and R. A. Serota: Phys. Rev. B **44** (1991) 8858.
  - [20] H. Yoshioka: Ph.D. thesis, Univ. of Tokyo (1992). H. Yoshioka and H. Fukuyama: *Transport Phenomena in Mesoscopic Systems, Springer Series of Solid State Sciences*, ed. H. Fukuyama and T. Ando (Springer, Berlin, 1992) 263.
  - [21] L. D. Landau and E. M. Lifshitz: *Statistical Physics, Part 1* (Pergamon, Oxford, 1980) §60.

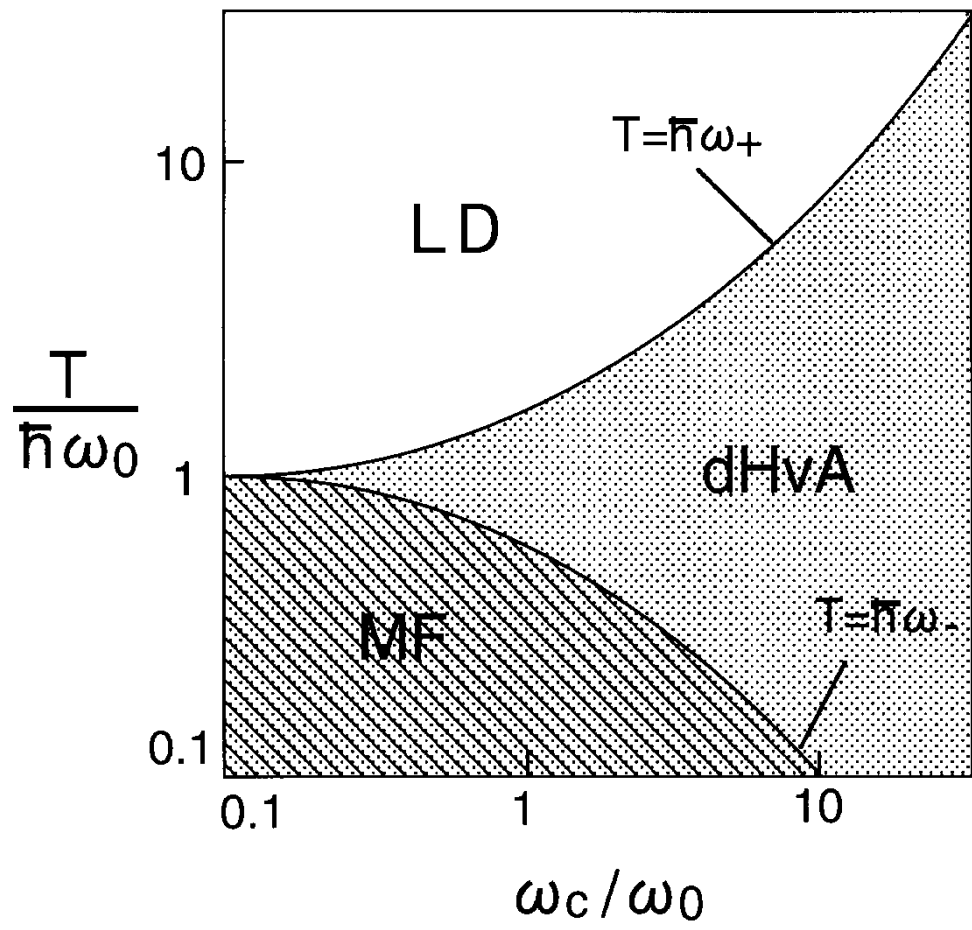
Fig. 1. Phase diagram showing characteristic regions of the field dependence of magnetic moment at various temperatures.

Fig. 2. Magnetic field dependences of magnetic moment at various temperatures. The dependences under a weak field ( $\omega_c \lesssim \omega_0$ ) are shown in (a) and (b), where (a) corresponds to “MF” and (b) ranges from “MF” to “LD”. On the other hand, the dependences under a strong field ( $\omega_c \gtrsim \omega_0$ ) are shown in (c) and (d), where (c) and (d) range from “MF” to “dHvA” and from “dHvA” to “LD”, respectively. The number of electrons is fixed to 5000.

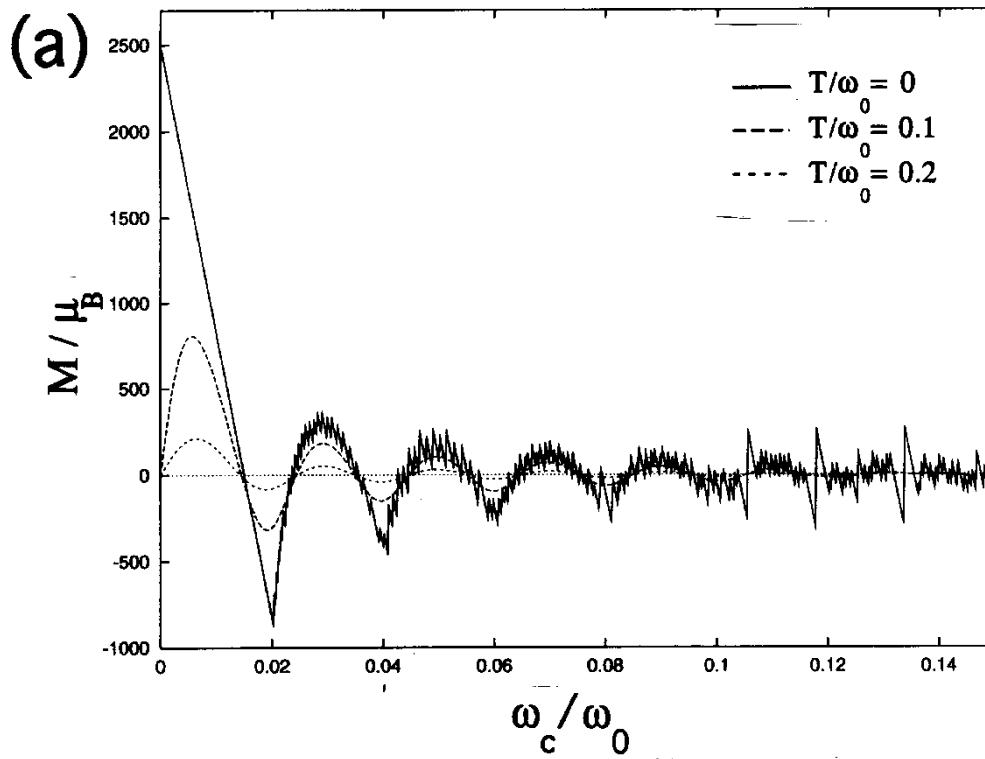
Fig. 3. A schematic illustration of the current flowing in the system.  $J_\theta(r)$  is defined positive in the direction as here.

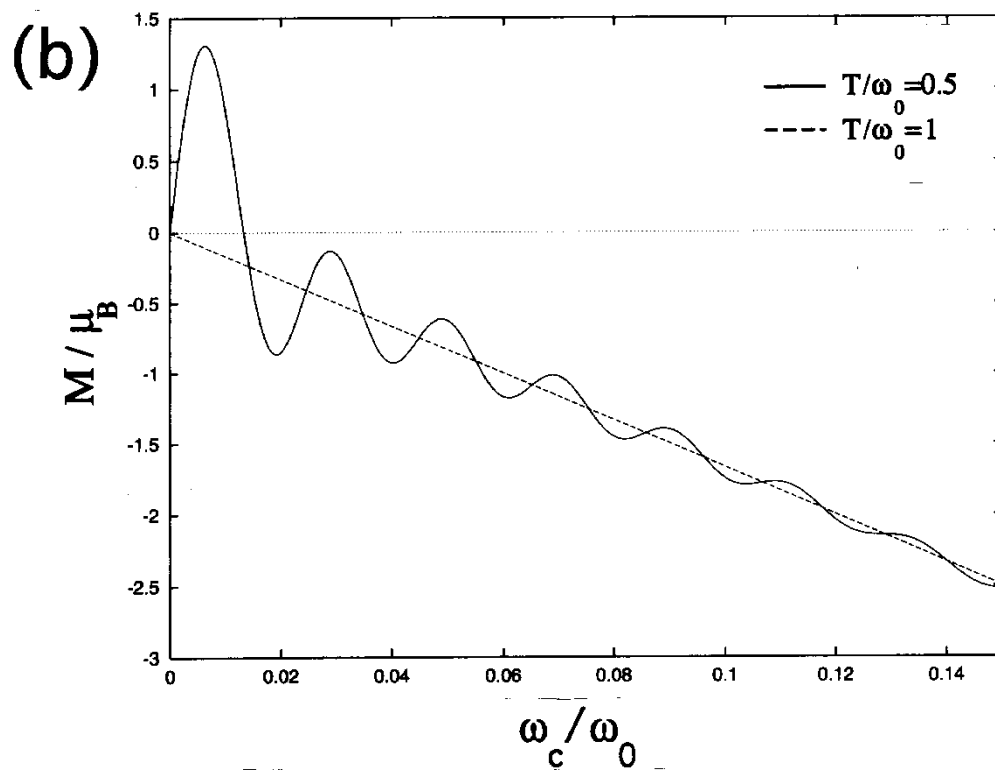
Fig. 4. Spatial distribution of current at various temperatures. Here, (a) and (b) are the current distribution under a weak field ( $\omega_c/\omega_0 = 0.1$ ), where (a) corresponds to “MF” and (b) ranges from “MF” to “LD”. (c) and (d) are the current distribution under a strong field ( $\omega_c/\omega_0 = 20$ ), where (c) and (d) range from “MF” to “dHvA” and from “dHvA” to “LD”, respectively. The number of electrons is fixed to 5000.  $J_\theta(r)$  is normalized by  $j_0 = e\omega_0/4\pi\xi$ .

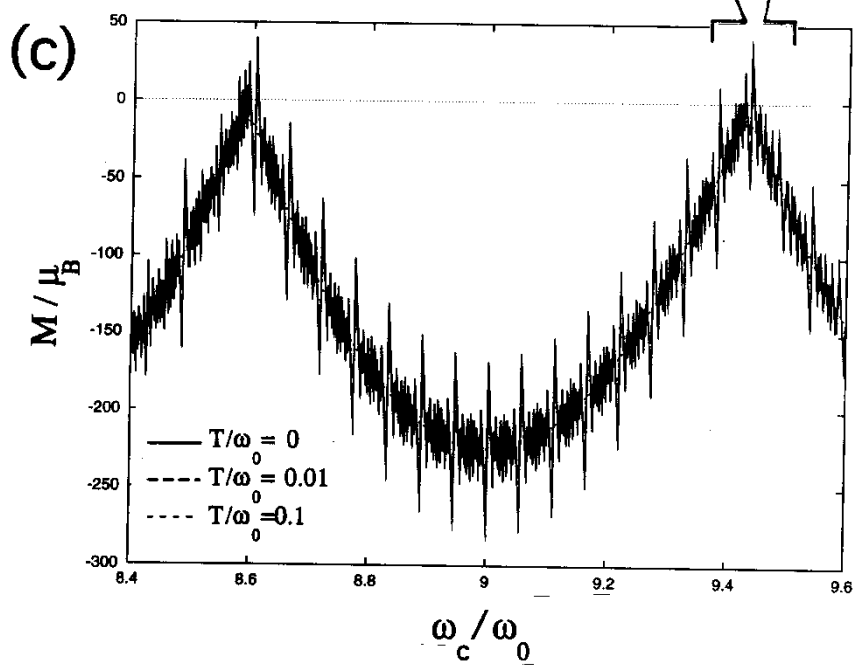
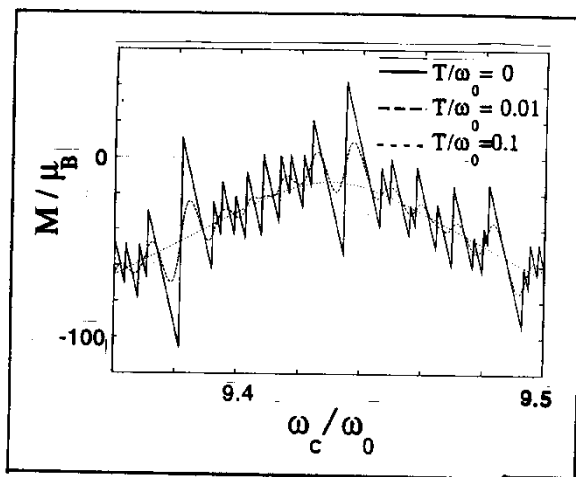
Fig. 5. A schematic illustration of the reflection at the boundary confining potential; (a)  $l_c(= \hbar v_F/\pi T) \gtrsim L$  where the multiple reflection becomes dominant, and (b)  $l_c \lesssim L$  where the boundary affects the behaviors of electrons only around the boundary.

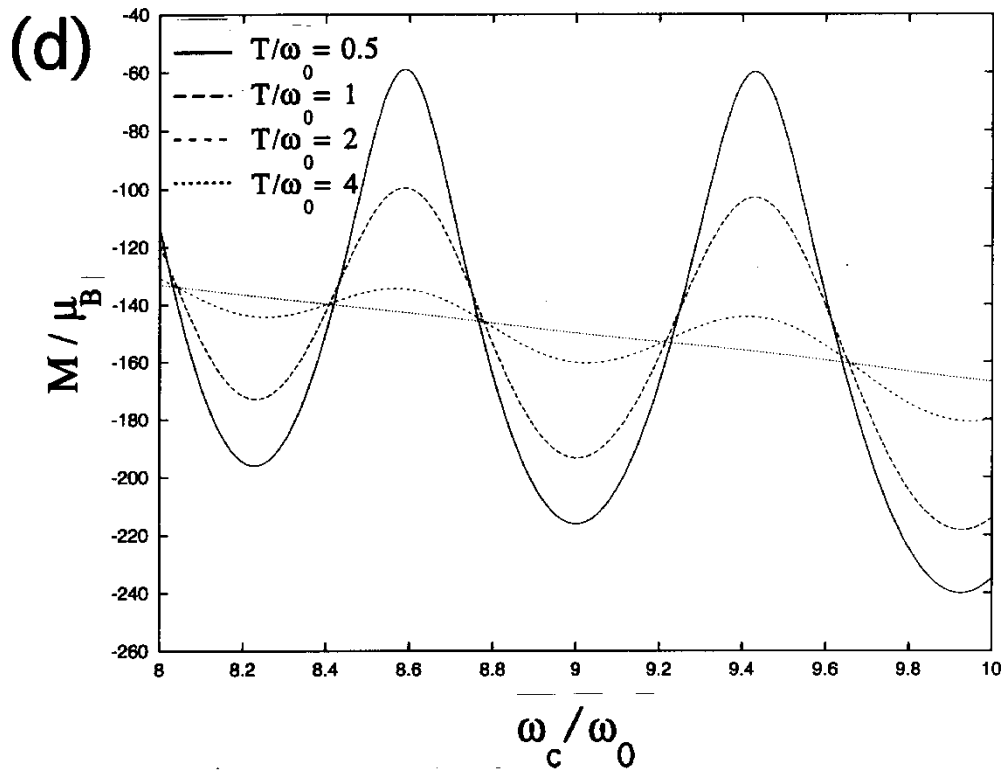


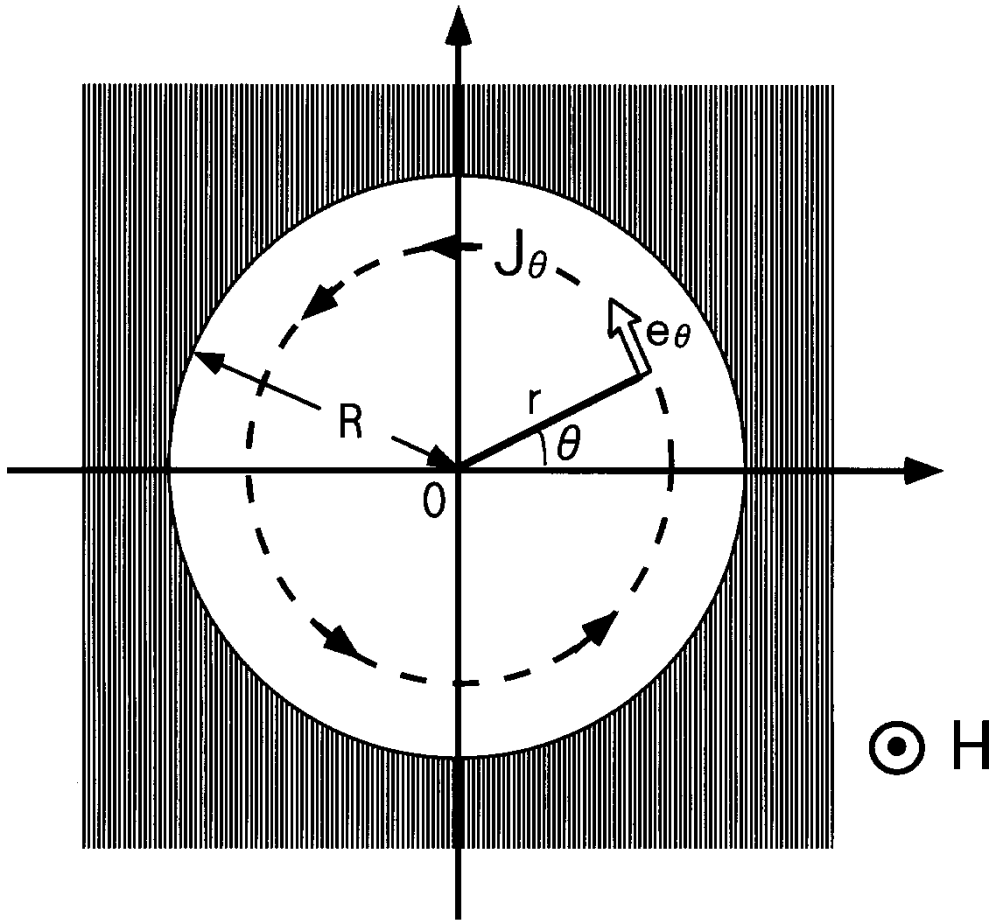


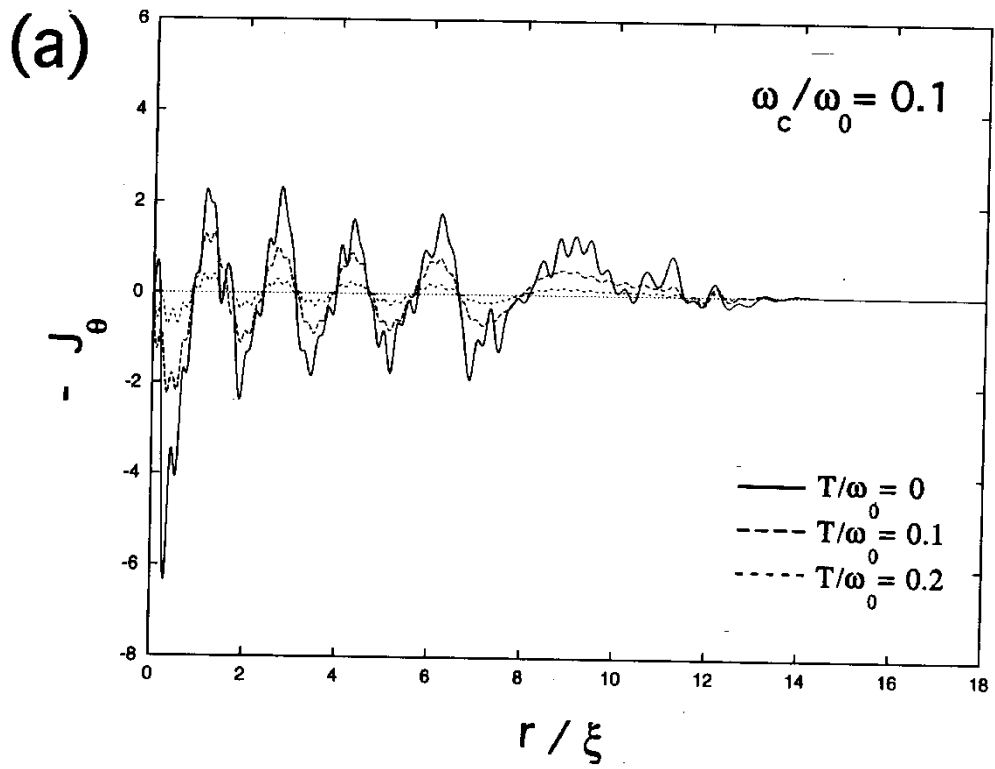


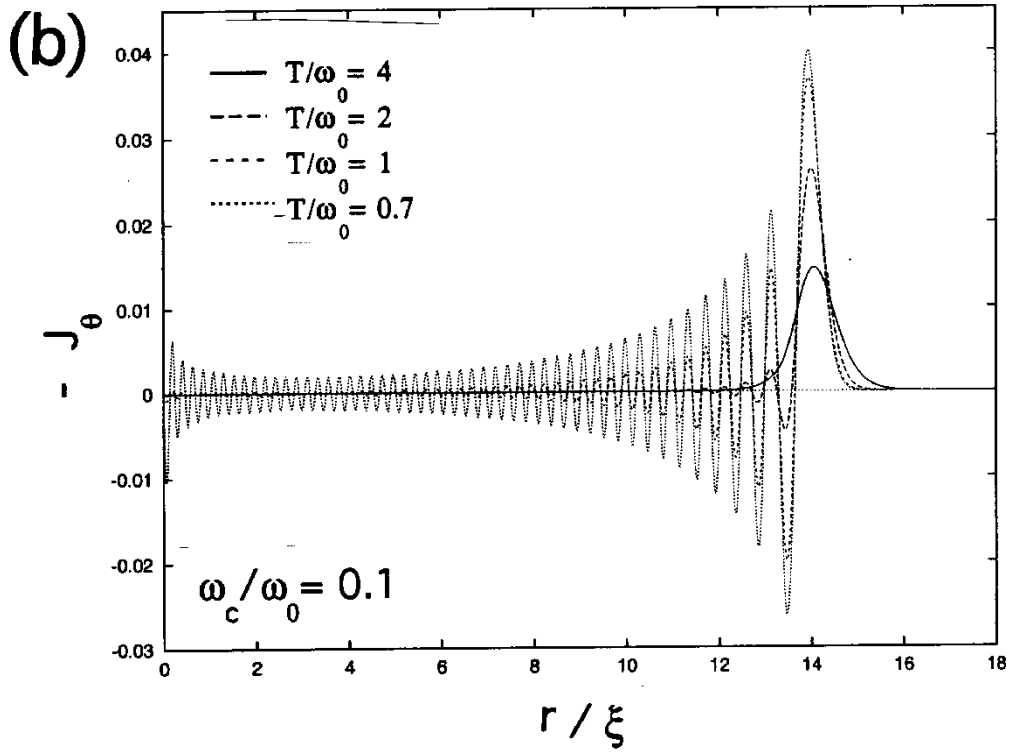


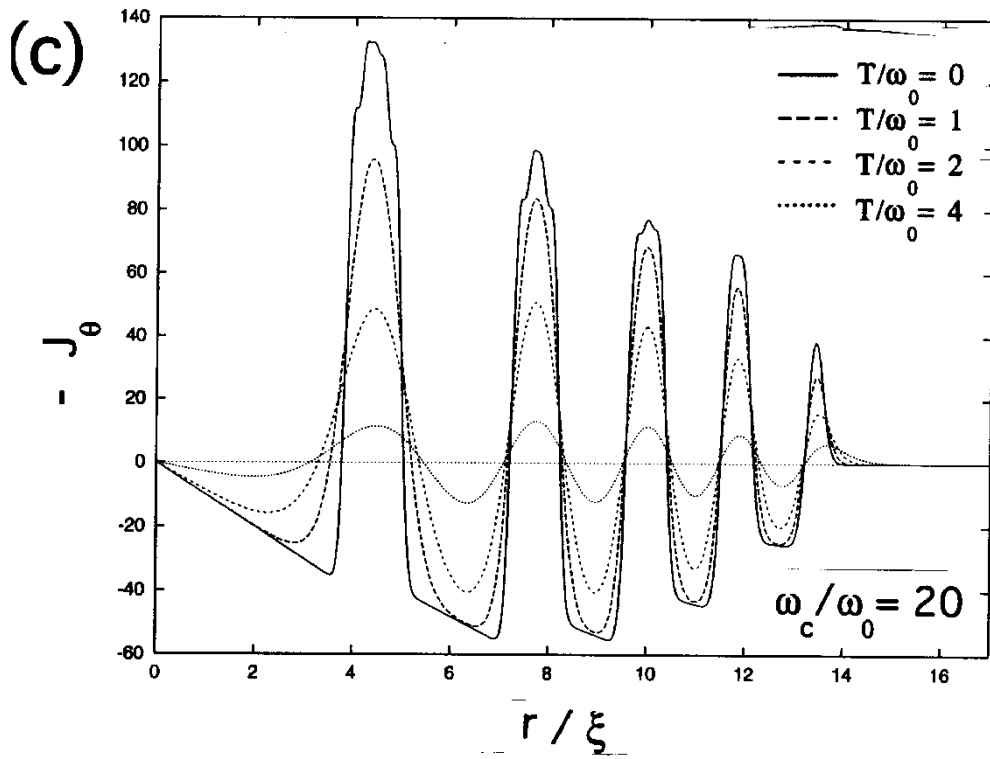






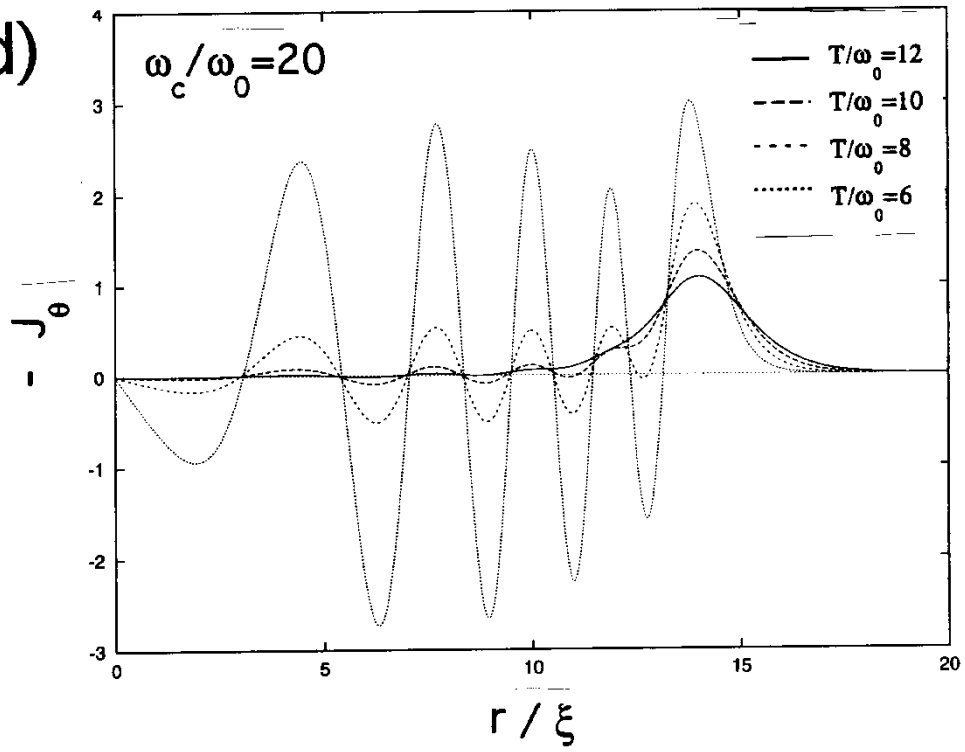






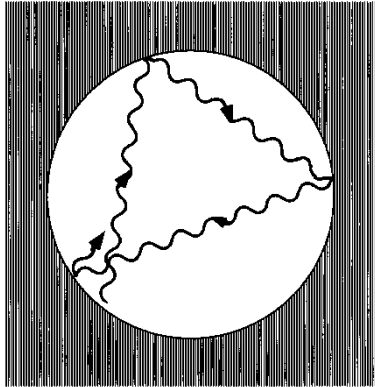


(d)



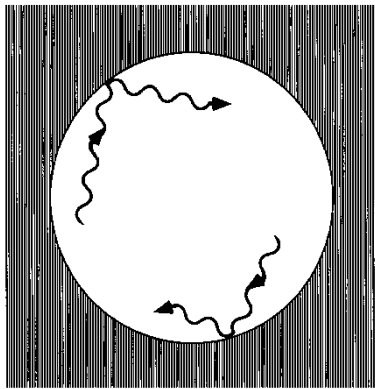
(a)

$\longleftrightarrow L \longrightarrow$



$l_c \gtrsim L$

(b)



$l_c < L$